

Fast charging nickel-metal hydride traction batteries

Xiao Guang Yang, Bor Yann Liaw^{*}

Hawaii Natural Energy Institute, School of Ocean and Earth Science and Technology, University of Hawaii at Manoa, 2540 Dole Street, Holmes Hall 246, Honolulu, Hawaii 96822, USA

Received 11 December 2000; received in revised form 26 December 2000; accepted 26 December 2000

Abstract

This paper describes the fast charge ability, or “fast rechargeability”, of nominal 85 Ah Ni–MH modules under various fast charge conditions, including constant current (CC); typically 1–3C, and constant power (CP) regimes. Our tests revealed that there is no apparent difference between CC and CP fast charge regimes with respect to charge efficiency and time. Following the USABC Electric Vehicle Battery Test Procedures Manual (Revision 2, 1996), we demonstrated that we were able to return 40% state of charge (SOC) from 60% depth of discharge (DOD) to 20% DOD within 15 min. Most importantly, we found that the internal pressure of the cell is the most critical parameter in the control of the fast charge process and the safe operation of the modules. © 2001 Elsevier Science B.V. All rights reserved.

Keywords: Fast charge; EV battery; Nickel metal hydride batteries; Charge algorithm; Internal pressure control; Charge efficiency

1. Introduction

Electric and hybrid vehicles (EHVs), an emerging automotive technology today, are designed for better fuel economy and zero or ultra-low emission. As early as 1996, a specially designed EV powered by an Ovonic Ni–MH battery pack achieved a driving range of 600 km on a single charge. Despite the great potential of solving the limited range problem, the cost of the battery pack remains to be a major barrier to commercialization. At the present time, most of the automakers favor a hybrid vehicle, in which a compact internal combustion engine (ICE) provides the base-load power while a small battery pack provides additional power necessary for acceleration and hill climbing or absorbing excess power by capturing the energy from the regenerative braking. The Ni–MH battery has been considered to be one of the most promising candidates in a hybrid electric vehicle application because of its high-power capability, long cycle life and no memory effect. Although attractive, the Ni–MH system still needs to be proved that it can be rapidly recharged for various reasons. For example, in an EV configuration, rapid recharge can greatly improve the vehicle’s mobility and usability and allow the vehicle operator to fully utilize the battery capacity without exceeding the range limit. For hybrids applications, the ability of

high power recharge can simplify power control algorithms and improve efficiency to capture regenerative braking power.

Fast charging presents certain merits for all types of batteries. One obvious reason is: the shorter the recharge time, the more convenience the user enjoys. There are other considerations in vehicle applications. For example, the performance of a battery in a dynamic field operation demands proper integration with the drive system. Fast rechargeability can facilitate the vehicle operation. Thus, improving our understanding of how the battery performs under high-rate vehicle operating conditions, including high-rate charging, will significantly enhance the performance and life of the battery and lower its overall cost of ownership. Therefore, the development of effective charge algorithms not only can reduce charging time, increase energy efficiency but also can overcome some limitations impeding the market acceptance of EHVs.

Successful experiences on fast charge have been achieved on valve-regulated lead-acid (VRLA) batteries and packs [1–5]. For instance, the Advanced Lead Acid Battery Consortium (ALABC) has set out plans to explore the realistic limitations on fast charging of VRLA batteries. Its ambitious goals are: (i) to return 50% of charge in not >5 min; (ii) to return 80% of the nominal 3 h capacity within 15 min; (iii) to fully recharge the battery within 4 h. Few VRLA battery manufacturers have met these goals [6]. A prevailing charging technique is to monitor the resistance-free voltage of the battery, V_{RF} , to ensure proper fast charge of the battery,

^{*} Corresponding author. Tel.: +808-956-2339; fax: +808-956-2335.
E-mail address: bliaw@hawaii.edu (B.Y. Liaw).

thus, yielding desired charging efficiency and minimizing temperature rise [7]. Fast charging, typically at charge rates over 25 kW, is however not meant to charge the battery pack to 100% SOC. Rather, fast charging should be terminated when the battery is no longer sustaining fast charge at such a high rate. It occurs typically >70–80% SOC, depending on the battery technology.

Fast charge remains a real challenge for the Ni–MH traction batteries. Most Ni–MH batteries are not recommended for fast charge [8] due to the concern that significant heat (I^2R) will be generated from the inherently higher impedance of the system than other chemistries. Therefore, liquid cooling of the battery modules is one of the enabling technologies for fast charging of Ni–MH batteries. But, so far limited work has been reported on fast charge of Ni–MH batteries or modules, especially for the electric vehicle applications. Knowledge of the fast-charge control of the Ni–MH batteries (especially, the traction batteries) and their operating limits and underlying mechanisms is therefore crucial to proper utilization and operation of such devices.

2. Experimental aspects

2.1. Experimental set-up

The test modules were made of 11 Ni–MH cells, giving a nominal voltage of 12 V.

The nominal capacity of the test module was rated at $C/3 = 85$ Ah and $C/1 = 80$ Ah. The physical dimensions of each individual module are 102 mm (W) \times 179 mm

(H) \times 410 mm (L). The batteries were sealed in a stainless steel casing with a gas vent that could be easily tapped with a pressure gauge, essential for the control of the charge process.

In all tests, the module was placed in a test box provided by the battery manufacturer. The test box comes with a small electrical cooling fan installed on the baseboard at the bottom of the box. Through a wind tunnel the fan forces cool air to pass through the module upward to improve heat dissipation and temperature control. All tests were conducted in an air-conditioned room where the ambient temperature was controlled in the range of 23–25°C.

All fast charge tests were conducted using an AeroVironment ABC-150 battery cycler with a designated National Instruments data acquisition system (primarily consisting of an SCXI-1121 signal conditioning unit and a PCI-MIO-16XE-50 NIDAQ board) to continuously monitor the module voltage, temperature, and internal pressure of one of the 11 individual cells. Fig. 1 illustrates the layout of the experimental set-up. The temperature was measured by attaching a thermocouple (Omega Engineering, Inc., Stamford, Connecticut) at the middle of the sidewall of the center cell casing inside the thermal control box. The internal gas pressure was monitored by a pressure gauge made by Measurement Specialties, Inc., Fairfield, New Jersey. The relative pressure range readable by the gauge and the data acquisition system was 160 psi or 10.9 atm. The signals monitored by the data acquisition system were also used in the control of the charging process through the NIDAQ interface supported by the Remote Operation System of the ABC-150 cycler.

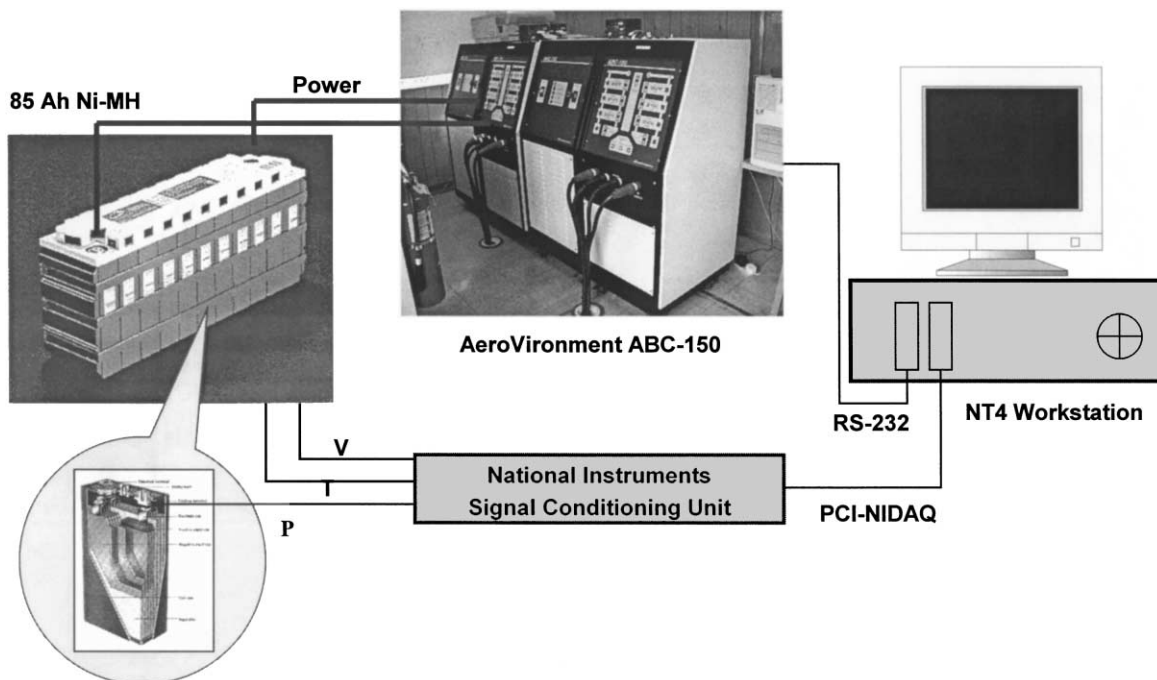


Fig. 1. Schematic of the experimental set-up.

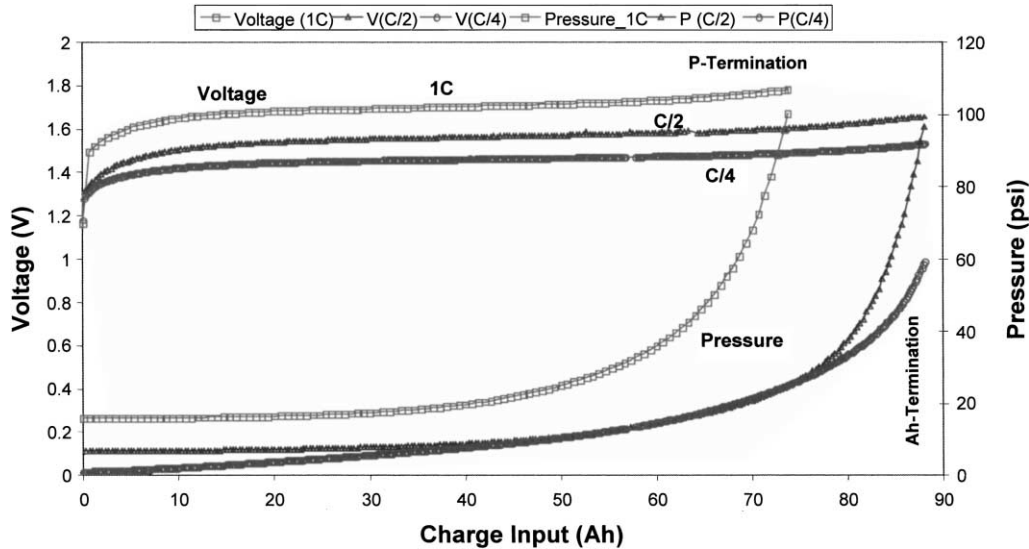


Fig. 2. Voltage and pressure profiles vs. charge input in various constant current (CC) charging regimes. The significant increase in pressure with charge rate depicts the importance of pressure control in fast charge.

2.2. Test protocols

The charge test protocols include constant current (CC) and constant power (CP) charging regimes. The CC charge rate ranges from 1 to 3 C, which corresponds to 85–255 A. In the CP charge regimes, the applied power levels were 1.49, 2.5, and 5.3 kW, which roughly correspond to the average power used in the 1, 1.6 and 3 C charge tests, respectively. We also conducted normal cycle tests at slower charge and discharge rates for comparison.

Generally, we first discharged the module at $C/3$ rate to the desired state of charge (SOC), and then recharged it in different charge regimes. The capacity return of the module was evaluated at the $C/3$ rate (-28.3 A) for comparison.

Following the DOE/USABC Electric Vehicle Battery Test Procedures Manual (Revision 2, 1996) [9], we also conducted Procedure #12 — fast charge tests. Each test cycle is consisted of the following four steps:

1. The first step involves recharging the module at $C/4$ rate to its full capacity.
2. The second step is a controlled discharge to drain the capacity to 60% depth of discharge (DOD).
3. The third step involves recharging the module using various fast charge regimes to evaluate module's capability of restoring charge from 60 to 20% DOD within 15 min.
4. The fourth step is a $C/3$ discharge to determine the capacity and SOC return.

In all charge tests, the module voltage, temperature, pressure, and charge input were monitored, recorded, and controlled to ensure a proper termination was achieved. In the fast charge tests, we found that the primary controlling parameter is the internal cell pressure, which has a profound impact on the battery performance.

Fig. 2 shows the reason why the pressure control is so important in the control of the high rate recharges. The voltage and pressure profiles shown in Fig. 2 depict the pressure change of the module under different charge rates as a function of the charge input. In the conventional low-rate charge regimes, such as those with rates lower than $C/2$, the charge process was typically terminated by voltage, temperature change, or even charge input (AhIn) cut-off. Under these circumstances, the pressure buildup in the cell is usually below the pressure limit of the vent, thus not critical for termination control. As the charge rate increased the gas evolution rate increased as well, resulting in a substantial pressure buildup in the cell. The pressure buildup became critical when the charge rate was above $C/2$. To avoid overcharging and venting, the pressure control in the regimes over $C/2$ thus are the predominant consideration.

3. Test results

3.1. The low rate charging test

For the purpose of constructing a baseline comparison, we first present the test under a low charging rate. Fig. 3 shows all the test profiles of the 85 Ah Ni–MH module cycled at $C/4$ (20 A) rate charging and $C/3$ (28.4 A) discharging to 11 V. The test was terminated at an input charge of 87.9 Ah. The module then delivered a capacity of 84.7 Ah with a Coulombic efficiency of 96.4%. The charge loss was assumed primarily due to the self-discharge reaction during the cycle. The associated energy input and output were 1.384 and 1.145 kWh, respectively, resulting in a round-trip energy efficiency of 82.7%. The internal pressure profile, shown in Fig. 3, shows that the gassing rate increased as the charge process progressed. At the end of the charge, the pressure

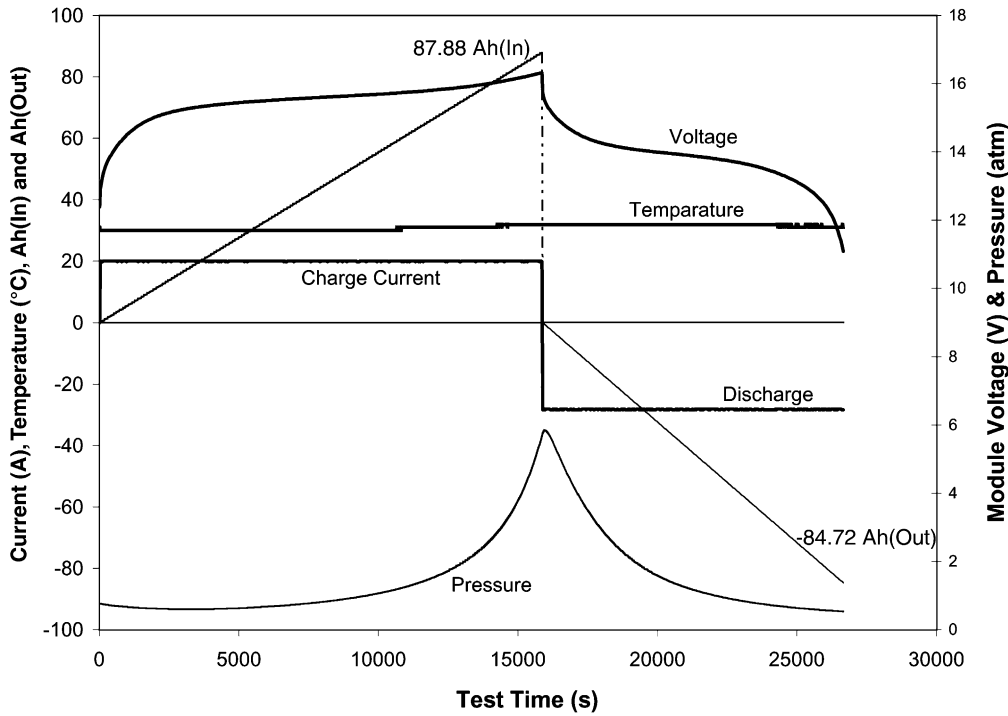


Fig. 3. Charge characteristics and profiles of a nominal 85 Ah Ni–MH traction battery module cycled at $C/4$ charge with charge input control and $C/3$ discharge to 11 V.

reached the maximum at 5.77 atm (or 85 psi). The pressure decline upon discharge implies that either the electrodes have absorbed the gas components as the surface concentrations of the active species decreased or the gas species took part in the cell reaction during the discharge. The temperature rise was moderate, about 2°C during the charge regime.

3.2. High-rate recharge from the discharged state

3.2.1. Constant current (CC) charging

In contrast to the low rate charging, we conducted a series of rapid CC charging under different rates ranging from 1 to 3 C. Fig. 4 shows typical cycle profiles of a test module under 1.6 C (136 A) charge regime with a ventlid pressure

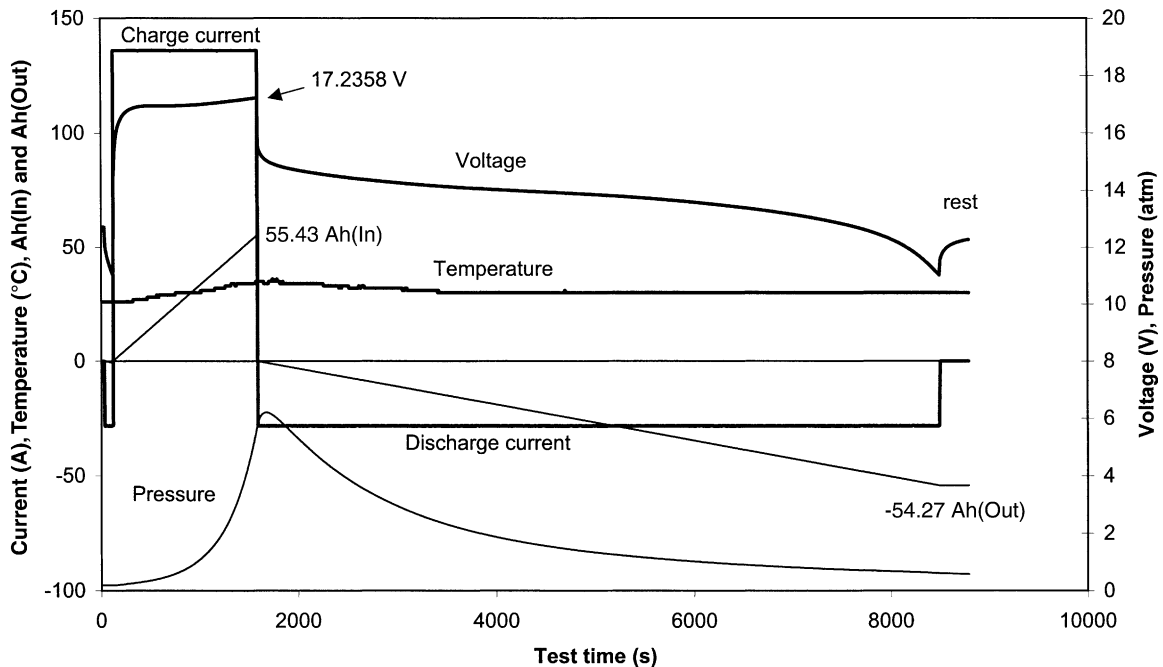


Fig. 4. Typical charge characteristics and profiles of the same Ni–MH module under 1.6 C charge with pressure control and $C/3$ discharge to 11 V.

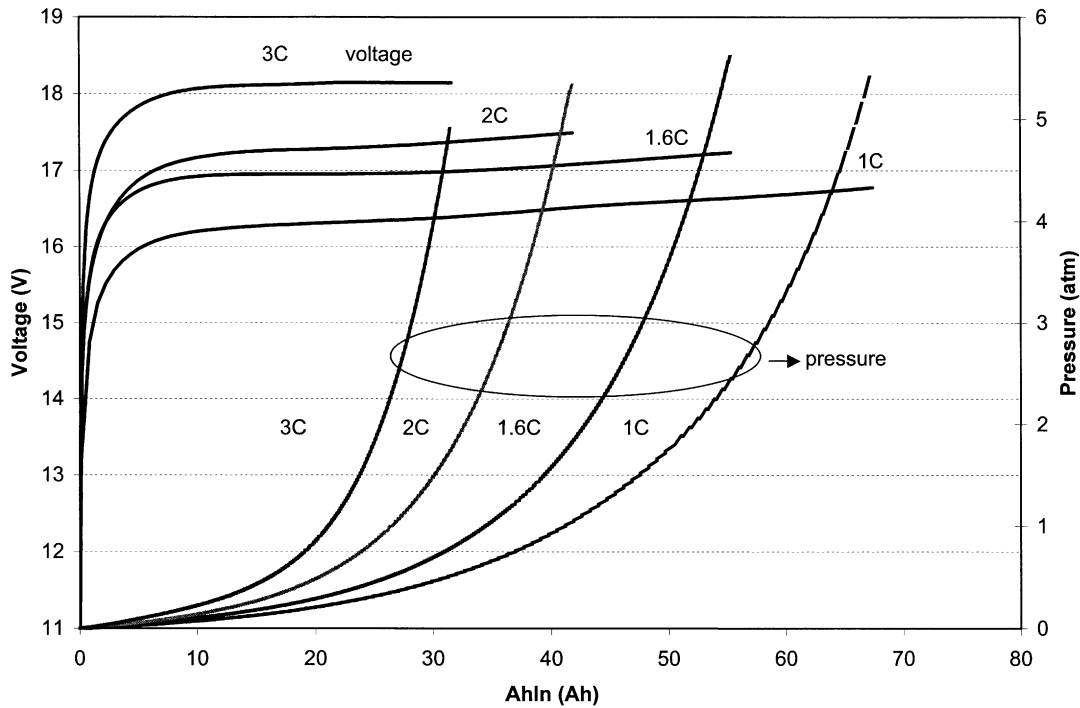


Fig. 5. Voltage and pressure profiles of the test module under different constant current charge regimes ranging from 1 to 3 C.

set at 6.8 atm. The Coulombic efficiency and energy efficiency for the 1.6 C rate test were calculated to be 97.9% (54.4 Ah/55.4 Ah) and 71.7% (0.734 kWh/1.023 kWh), respectively. The high rate charge tests suggest that, as the charge current increased, the Coulombic efficiency remained high, while the energy efficiency declined.

Fig. 5 summarizes the voltage and pressure profiles of a test module as a function of charge input (AhIn) under different CC charge rates ranging from 1 to 3 C. The charge processes were all terminated by the pressure lid around 6 atm or 85 psi. The amount of charge return is however reduced as the charge rate increased. In each charge regime, the pressure increased exponentially with charge input before the cut-off.

3.2.2. Constant power (CP) charging

We investigated fast charge performance under three CP regimes in an attempt to distinguish the difference, if any, between CC and CP charging. Fig. 6 shows the current profiles of a Ni–MH module with respect to charge input (AhIn) under these CP charge regimes. In all the three cases, the initial charge current was high but quickly stabilized at a lower level and remained relatively constant afterwards. In the 1.49 kW regime, the current decreased to 85 A shortly after the initiation of the charge process and stayed roughly constant throughout the rest of the charging period. In the 2.50 kW regime, the current plateau rested at 137 A. At 5.30 kW, the current level stayed around 250 A. Thus, the power levels asserted in the tests, 1.49, 2.5 and 5.3 kW, roughly correspond to the average charge rate of 1, 1.6 and

3 C, respectively. The resulting charge characteristics are therefore comparable to those of the CC charging regimes.

Fig. 7 shows the comparison of the charge input (AhIn) and capacity (AhOut) with respect to charge duration under various CC and CP regimes. According to the test results, the highest degree of “rechargeability” was achieved with about 37% SOC return in 8 min. In Table 1, we summarize the AhIn, AhOut, recharge time, temperature rise and the maximum module voltage in these recharge regimes. For 1, 1.6, 2 and 3 C recharging, the capacity of the module returned from its fully discharged state to around 75, 62, 48 and 36% SOC, respectively. In Table 1, we found that the

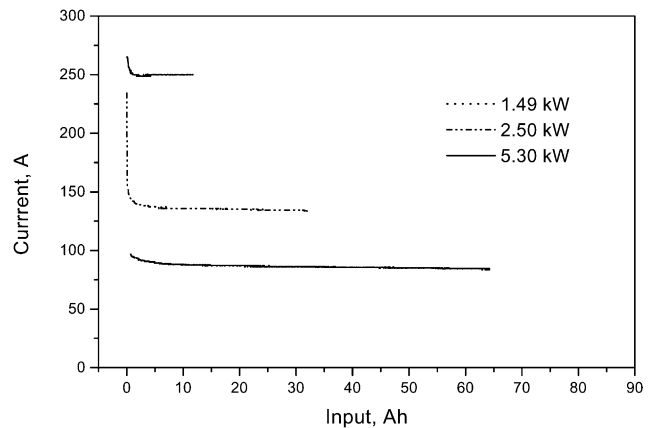


Fig. 6. Current vs. charge input (AhIn) of the Ni–MH module under various constant-power fast charge regimes.

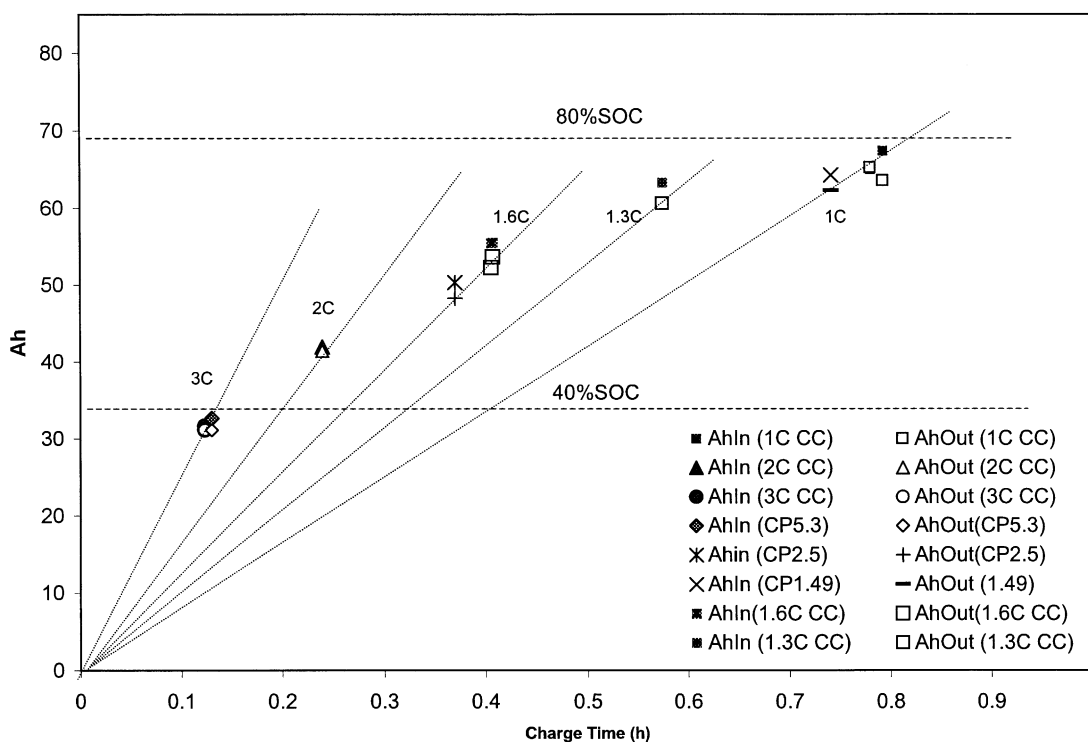


Fig. 7. Comparison of charge input (AhIn) and capacity (AhOut) with respect to charge duration under various constant current and constant power regimes.

temperature rose by about 10–11°C when the module was charged at about 3 C rate. Inevitably, the temperature rise could appreciably affect the extent of charge return of the electrodes. According to the pressure–composition–temperature (*p-c-T*) curve of most metal hydride systems, we often found that the equilibrium partial pressure of hydrogen usually increased while the hydrogen content in the hydride remained constant, with temperature. As a consequence, the temperature escalation will result in increased hydrogen gassing and venting, as well as reduced capacity. This effect could limit the charge acceptance and the return of charge at

high rates, not to mention the loss of the electrolyte and potential dryout. To mitigate this effect, a proper thermal management seems to be the key. If we could actively control the module temperature, a higher percentage of charge return and a higher recharging rate could be achieved.

In the present paper, we did not account for the effect of electrolyte concentration on the battery behavior. However, a detailed individual electrode potential characterization and analysis of the gas composition are all critical to the elucidation of the mechanism. More systematic study is obviously required to understand this behavior.

Table 1
Summary of the fast charge results of the Ni–MH modules under various charge regimes

Charge regime	AhIn (Ah)	AhOut (Ah)	Efficiency (%)	SOC (%)	Charge time (h)	ΔT (°C)	V-term (V)
Constant current (C)							
1	67.4	63.55	94.3	74.8	0.793	3	16.778
	65.03	65.22	100	76.7	0.781	4	16.734
1.6	55.44	52.27	94.3	61.5	0.406	8	17.236
	55.55	53.65	96.6	63.1	0.408	7	17.308
2	41.99	41.44	98.7	48.7	0.239	8	17.491
	31.66	31.04	98.0	36.5	0.123	9	18.144
3	31.12	31.13	100	36.6	0.123	10	18.119
	Constant power (kW)						
1.49	64.24	62.27	96.9	73.3	0.742	4	16.746
2.50	50.34	48.32	96.0	56.8	0.370	7	17.166
5.30	32.64	31.14	95.4	36.6	0.130	11	18.157

3.3. Fast charging from different initial SOC's

We conducted a set of tests using constant-current charging at 1, 1.6, 2, 2.3, 2.7 and 3 C rates to investigate the dependence of charge characteristics from different initial SOC, i.e. 0, 20, 40 and 60%. In these tests, we extended the pressure lid to 10 atm. Fig. 8 shows the charge input (AhIn), capacity (AhOut), and the terminal SOC determined by the subsequent C/3 discharge in the above four series of tests. For a set of the same initial SOC tests, the capacity increases logarithmically with the recharging time at different rates and as terminated by the same pressure lid. For instance, in the case of starting from an initial 40% SOC, the terminal SOC at the 3 C rate is 72%; 92% SOC at 1 C, etc. according to the following equation:

$$SOC_{(\text{Terminal at } 40\% \text{ init; } 10 \text{ atm; } 25^\circ\text{C})} = 12.5 \ln(t_{\text{charge_max at } n \text{ C, min}}) + 48.7(\%SOC)$$

where $t_{\text{charge_max at } n \text{ C}}$ depicts the maximum charge duration for the specific $n \text{ C}$ ($n = 1-3$) charge rate at 25°C and terminated by the pressure lid of 10 atm. The results can be further summarized in Fig. 9, where the terminal SOC contours are plotted against the initial SOC and the charge rate. This figure shows the map of how to estimate the capacity in the fast charge regimes if the initial SOC and charge rate are known and with the pressure lid control.

3.4. Fast charge evaluation following the USABC criteria and guidelines

The purpose of this test is to evaluate the fast rechargeability of the Ni–MH modules according to the USABC criteria and guidelines. Accordingly, we successfully returned 40% SOC to an 85 Ah Ni–MH traction battery module in 15 min, as shown in Fig. 10. In this particular test, we showed that in the pre-test cycle we were able to charge

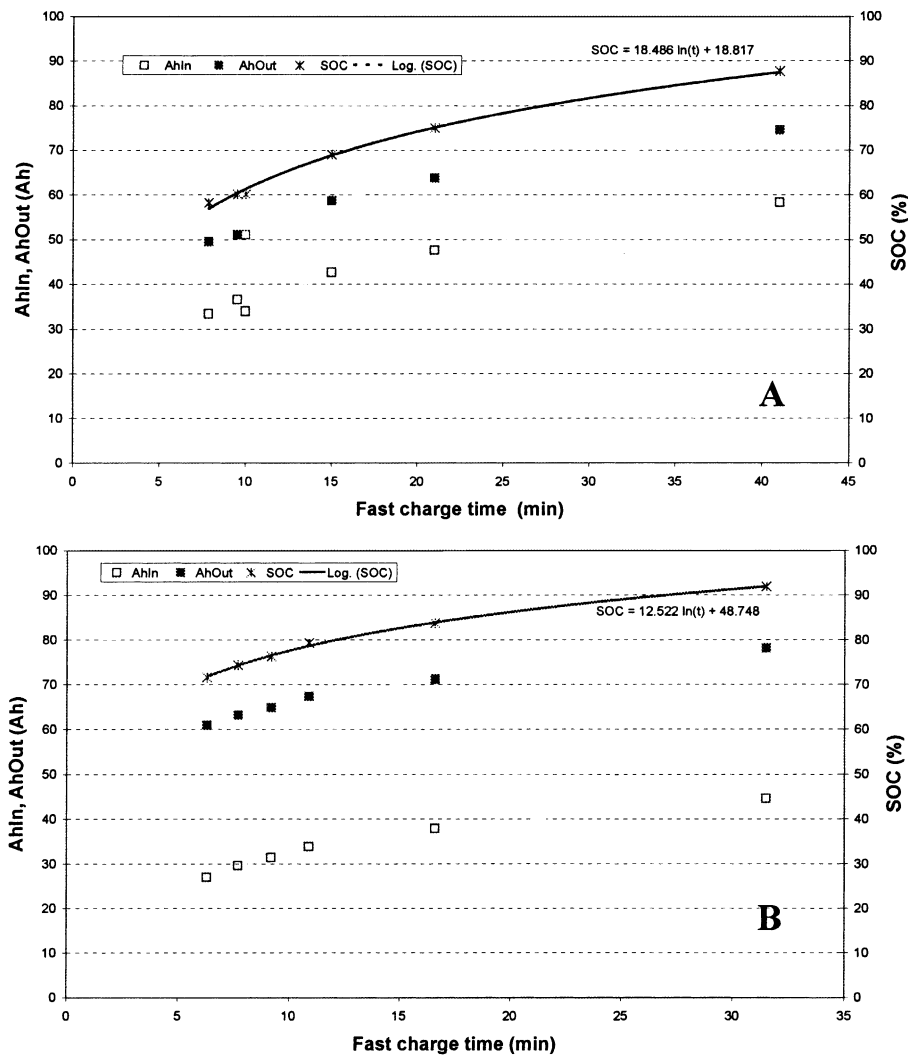


Fig. 8. The charge input and capacity return in various constant current charging regimes from various initial states of charge (SOC). The initial SOC's are: (A) 0%; (B) 20%; (C) 40%, and (D) 60%.

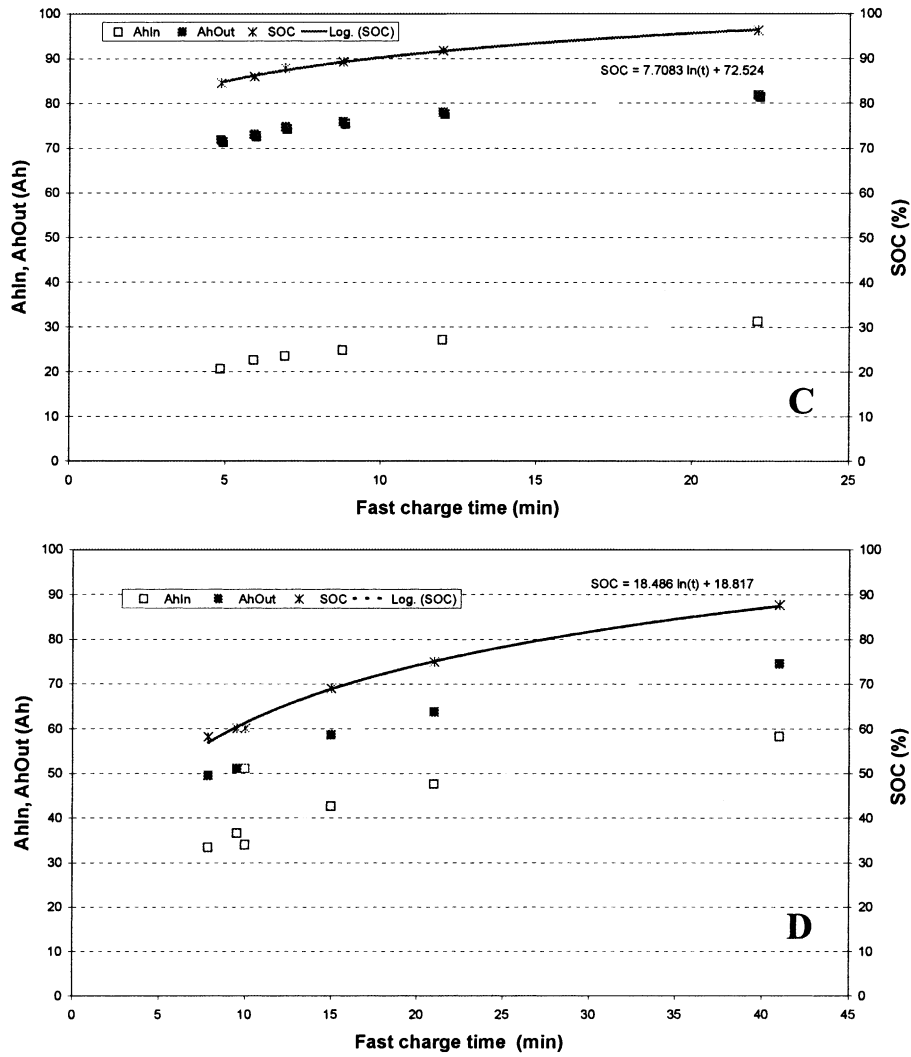


Fig. 8. (Continued)

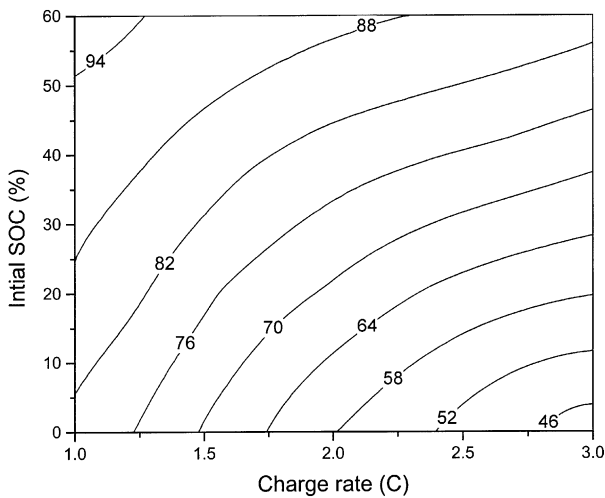


Fig. 9. Summary of the fast charge results: the terminal SOC as a function of the initial SOC and charge rate at 25°C with pressure termination at 10 atm.

the module with 87.88 Ah and return 84.72 Ah of capacity. In the following test cycle, we first charged the module at about $C/4$ rate to return 87.85 Ah. Subsequently, we discharged the module to 61% DOD by taking out 51.00 Ah at the $C/3$ rate. Then, we recharged the module at $CP = 2.5$ kW (similar for $CC = 1.6$ C) until 40% of the nominal capacity (35.03 Ah) has been reached. Finally, we discharged the module to 11 V at the $C/3$ rate. The result showed that 68.82 Ah was available at the end of discharge, which represents that 80% SOC was retained in capacity after the fast charge. During the constant-power or constant-current fast recharging, we found that the temperature increased from 29 to 34°C, and the maximum internal pressure only reached 4.5 atm. After this recharge test, no immediate degradation or damage to the module performance, such as capacity loss, was found. However, detailed study on the effects of fast charging on battery cycle life and the understanding of the mechanism of how the rapid charging affects the battery performance are necessary.

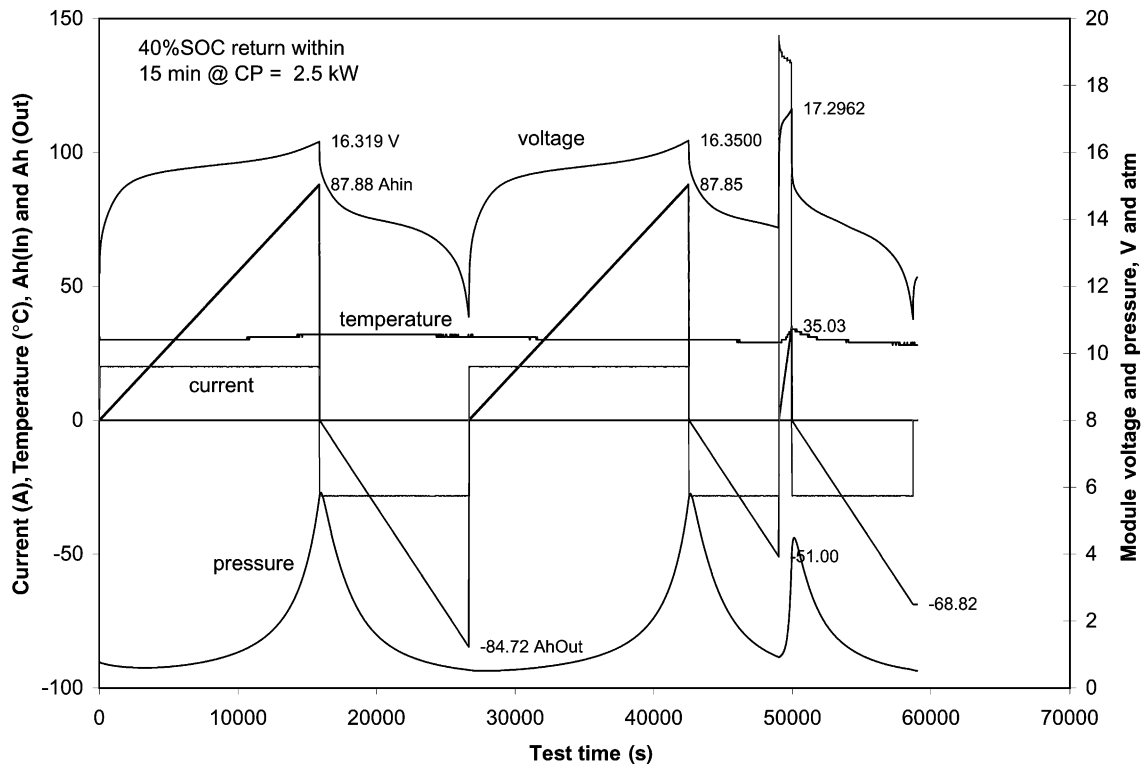


Fig. 10. The Ni–MH module subjected to the USABC fast charge test procedure, showing that it can return 40% of state of charge (SOC) from 60% depth of discharge (DOD) to 20% DOD within 15 min.

4. Conclusion

We conducted a series of fast charging tests on commercially available 85 Ah Ni–MH modules under different CC (1–3 C) and CP (1.49–5.3 kW) charge regimes from various initial states of charge (0–60%). The rapid rechargeability of these Ni–MH modules is exceeding the criteria set by the guidelines in the DOE/USABC EV Battery Test Procedure Manual. These Ni–MH modules can return 40% SOC from 60 to 20% DOD in 15 min using various fast charge regimes. We found that the Ni–MH modules could return 37% SOC in nearly 8 min, 50% SOC in 15 min, or 75% SOC in 48 min from the fully discharged state.

Acknowledgements

The authors would like to thank the Defense Advanced Research Projects Agency (DARPA) and the US Department of Transportation Advanced Vehicle Technology Program in

supporting this work under the Federal Cooperative Agreement MDA972-95-0009 with the Hawaii Electric Vehicle Demonstration Project (HEVDP).

References

- [1] T.G. Chang, E.M. Valeriote, D.M. Jochim, *J. Power Sources* 48 (1994) 163.
- [2] T.G. Chang, D.M. Jochim, *J. Power Sources* 64 (1997) 103.
- [3] M. Fernandez, F. Trinidad, *J. Power Sources* 67 (1997) 125.
- [4] D. Pavlov, G. Petkova, M. Dimitrov, M. Shiomi, M. Tsubota, *J. Power Sources* 87 (2000) 39.
- [5] S.C. Kim, W.H. Hong, *J. Power Sources* 89 (2000) 93.
- [6] P.T. Moseley, *J. Power Sources* 59 (1996) 81.
- [7] E.M. Valeriote, T.G. Chang, D.M. Jochim, in: *Proceedings of the 9th Annual Battery Conference on Applications and Advances*, Long Beach, California, 11 January 1994.
- [8] J.C. Kopera, *Fast Charging — Strategy for Success*, 1999.
- [9] USABC Electric Vehicle Battery Test Procedures Manual, Revision 2, DOE/ID-10479, Rev. 2, January 1996, Idaho National Engineering Laboratory.